Electronic Supplementary Information (ESI)

$RbPbPS_4$: a promising IR nonlinear optical material achieved by lone-pair-cation-substitution-induced structure transformation

A-Yang Wang,‡[a,b,c] Sheng-Hua Zhou,‡[a,d] Mao-Yin Ran,[a,b,e] Bingxuan Li,[a,b] Xin-Tao Wu,[a,b] Hua Lin,[*, a,b] and Qi-Long Zhu[*,a,b]

[a]*State Key Laboratory of Structural Chemistry, Fujian Institute of Research on the Structure of Matter, Chinese Academy of Sciences, Fuzhou 350002, China*

[b]*Fujian Science & Technology Innovation Laboratory for Optoelectronic Information of China, Fuzhou 350108, China*

[c]*College of Chemistry, Fuzhou University, Fuzhou 350002, China*

[d]*Resource environment & Clean energy Laboratory, School of Chemistry and Chemical Engineering, Jiangsu University of Technology 213001, China*

[e]*University of Chinese Academy of Sciences, Beijing 100049, China*

‡ A. Y. Wang and S. H. Zhou contributed equally to this work.

**E-mail: linhua@fjirsm.ac.cn and qlzhu@fjirsm.ac.cn*

Table of Contents

Electronic Supplementary Information (ESI)

Electronic Supplementary Information (ESI)

1 Experimental Section

1.1 Materials and Instruments

All reagents used in the present experiments were purchased from commercial sources and directly used without further purification. All weighing processes were completed in an anhydrous and oxygen-free glove box. The semi-quantitative energy dispersive X-ray (EDX, Oxford INCA) spectra were measured with a field emission scanning electron microscope (FESEM, JSM6700F). Powder X-ray diffraction (PXRD) analysis was carried out in a Rigaku Mini-Flex II powder diffractometer (Cu-K_α, λ = 1.5418 Å). UV-vis-NIR absorption measurement was performed in the region of 200−2500 nm at room temperature using an UV-vis-NIR spectrometer (Perkin-Elmer Lambda 950). The reflectance spectrum of the $BaSO_4$ powder was collected as the baseline and the diffuse reflectance data were converted to absorbance internally by the instrument by use of the Kubelka-Munk function.[1] The IR transmittance was measured on the PerkinElmer Spectrum One FT-IR Spectrometer in the range of 400−4000 cm^{-1}. The thermal stability analyses were measured on a NETZSCH STA 449C simultaneous analyser.

1.2 Synthesis

All reactants were stored and processed in a glove box filled with high-purity Argon. For the prepare of $RbPbPS_4$ crystals, mixtures of materials PbO (Macklin, 2.5N), P (Meryer, 2N), S (Aladdin, 4N), and B (Aladdin, 5N) in a molar ratio of 3:3:14:2, along with excess RbCl (Aladdin, 3N) serving as both a reactant and flux, were carefully weighed and loaded into a 13-mm quartz tube. This tube was placed in a computer-controlled muffle furnace after being flame-sealed at a vacuum of 10^{-4} Torr.. The heating procedure is as follows: first, raise the temperature to 673 K within

10 hours and maintain it at that temperature for 20 hours, then increase the temperature to 1023 K within 50 hours and hold it for 100 hours; finally, at a cooling rate of 3 K/h, shut down the tube furnace after the temperature drops to 623 K and allow it to cool naturally to room temperature. The target crystals appear light yellow (about 80% yield) and are mechanically separated from the products, which are rinsed with distilled water and ethanol. The title compound maintained its weight and color at room temperature more than 6 months, demonstrating its physical and chemical stability.

1.3 Single-Crystal Structure determination

Taking the high-quality crystal of $RbPbPS_4$ with suitable sizes was selected for single-crystal X-ray diffraction (XRD) analysis. The single-crystal diffraction data collections were collected on a Saturn 724 install with graphite-monochromated Mo-K_α radiation (λ = 0.71073 Å) at room temperature.The absorption correction was performed by the multi-scan method.[2] Using direct methods and maken further refinement by full-matrix least-square fitting on F^2 based on *SHELX−2014* software, the precise struture was determined sussessfully.[3] The atomic coordinates and equivalent isotropic of crystallographic information displacement parameters are given in the Tables 1 and S1. Bond distances (Å) and bond angles (°) of $RbPbPS_4$ are listed in Table S2. CIF of $RbPbPS_4$ has been submitted with CCDC number 2347371.

1.4 Second-Harmonic Generation (SHG) Measurements

The powder SHG property test was investigated by Kurtz-Perry method[4] using a Q-switched laser radiation. The laser radiation at 2900 nm was selected as the laser sources with the laser energy of 10 mJ and $AgGaS_2$ were measured as the benchmark,

respectively. Samples of $RbPbPS_4$ and $AgGaS_2$ were ground and sieved into different granule sizes (30−46, 46−74, 74−106, 106−150, and 150−210 μm) for the phase matching measurements. The frequency-doubled output signals were detected via photomultiplier tube and oscilloscope.

1.5 Laser Induced Damage Threshold (LIDT) Measurements

The LIDT of $RbPbPS_4$ at the maximal scope of 150−210 μm was carried out single pulse measurement method[5] and similar scope of $AgGaS_2$ single crystal used to the reference. The whole measuring materials were foist into selfsame plastic holders (thickness: 1 mm and diameter: 8 mm), respectively. Using an optical microscope monitor the exterior change of sample under the 1064 nm laser radiation with pulse width τ_p of 10 ns. Nova II sensor with a PE50-DIF-C energy sensor and a Vernier caliper was used for measuring the power of laser beam and the damage spot radius.

2 Computational Details

The DFT calculations have been performed using the *Vienna ab initio simulation package* (VASP)[6–8] with the Perdew-Burke-Ernzerhof (PBE)[9] exchange correlation functional. The projected augmented wave (PAW)[10] potentials with the valence states 5s and 5p for Rb, 6s , 6p and 5d for Pb, 3s and 3p for P, and 3s and 3p for S, respectively, have been used. A Γ-centered 9×7×7 Monkhorst-Pack grid for the Brillouin zone sampling[11] and a cutoff energy of 800 eV for the plane wave expansion were found to get convergent lattice parameters. The linear and nonlinear optical calculation was performed in the condition of a Monkhorst-Pack *k*-point mesh of 7×9×9.

Electronic Supplementary Information (ESI)

The imaginary part of the dielectric function due to direct inter-band transitions is given by the expression:

$$\varepsilon_2(\hbar\omega) = \frac{2e^2\pi}{\Omega\varepsilon_0}\sum_{k,v,c}\left|\left\langle\psi_k^c\left|u\cdot r\right|\psi_k^v\right\rangle\right|^2\delta(E_k^c - E_k^v - E) \quad \ldots\ldots\ldots\ldots (1)$$

where Ω, ω, u, v and c are the unit-cell volume, photon frequencies, the vector defining the polarization of the incident electric field, valence and conduction bands, respectively. The real part of the dielectric function is obtained from ε_2 by a Kramers-Kronig transformation:

$$\varepsilon_1(\omega) = 1 + (\frac{2}{\pi})\int_0^{+\infty} d\omega' \frac{\omega'^2\varepsilon_2(\omega)}{\omega'^2 - \omega^2} \quad \ldots\ldots\ldots\ldots (2)$$

The refractive index $n(\omega)$ can be obtained based on ε_1 and ε_2.

In calculation of the static $\chi^{(2)}$ coefficients, the so-called length-gauge formalism[12] derived by Aversa and Sipe[13] and modified by Rashkeev et al[14] is adopted, which has proven to be successful in calculating the second order susceptibility for semiconductors and insulators. In the static case, the imaginary part of the static second-order optical susceptibility can be expressed as:

$$\chi^{abc} = \frac{e^3}{\hbar^2\Omega}\sum_{nml,k}\frac{r_{nm}^a(r_{ml}^b r_{ln}^c + r_{ml}^c r_{ln}^b)}{2\omega_{nm}\omega_{ml}\omega_{ln}}[\omega_n f_{ml} + \omega_m f_{ln} + \omega_l f_{nm}] + \frac{ie^3}{4\hbar^2\Omega}\sum_{nm,k}\frac{f_{nm}}{\omega_{mn}^2}[r_{nm}^a(r_{mn;c}^b + r_{mn;b}^c) + r_{nm}^b(r_{mn;c}^a + r_{mn;a}^c) + r_{nm}^c(r_{mn;b}^a + r_{mn;a}^b)]$$

……(3)

where r is the position operator, $\hbar\omega_{nm} = \hbar\omega_n - \hbar\omega_m$ is the energy difference for the bands m and n, $f_{mn} = f_m - f_n$ is the difference of the Fermi distribution functions, subscripts a, b, and c are Cartesian indices, and $r^b_{mn;a}$ is the so-called generalized derivative of the coordinate operator in k space,

$$r^{b}_{nm;a} = \frac{r^{a}_{nm}\Delta^{b}_{mn} + r^{b}_{nm}\Delta^{a}_{mn}}{\omega_{nm}} + \frac{i}{\omega_{nm}} \times \sum_{l} (\omega_{lm} r^{a}_{nl} r^{b}_{lm} - \omega_{nl} r^{b}_{nl} r^{a}_{lm}) \quad \text{…… (4)}$$

where $\Delta^{a}_{nm} = (p^{a}_{nn} - p^{a}_{mm}) / m$ is the difference between the electronic velocities at the bands n and m.

As the nonlinear optical coefficients is sensitive to the momentum matrix, much finer k-point grid and large amount of empty bands are required to obtain a convergent $\chi^{(2)}$ coefficient. The $\chi^{(2)}$ coefficients here were calculated from PBE wave functions and a scissor operator has been added to correct the conduction band energy (corrected to the experimental gap), which has proven to be reliable in predicting the second order susceptibility for semiconductors and insulators.

Electronic Supplementary Information (ESI)

3 Figures and Tables

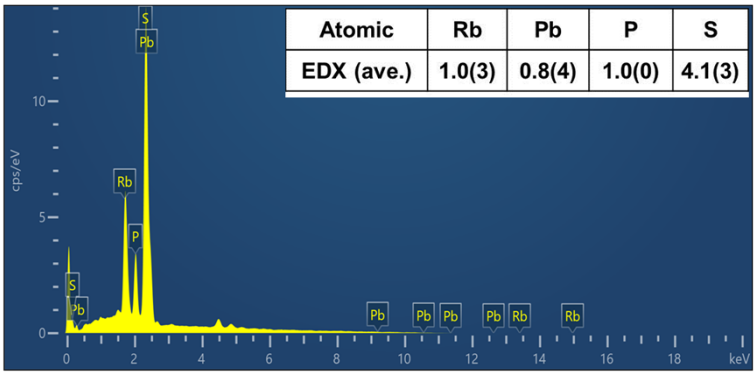

Figure S1. EDX results of $RbPbPS_4$.

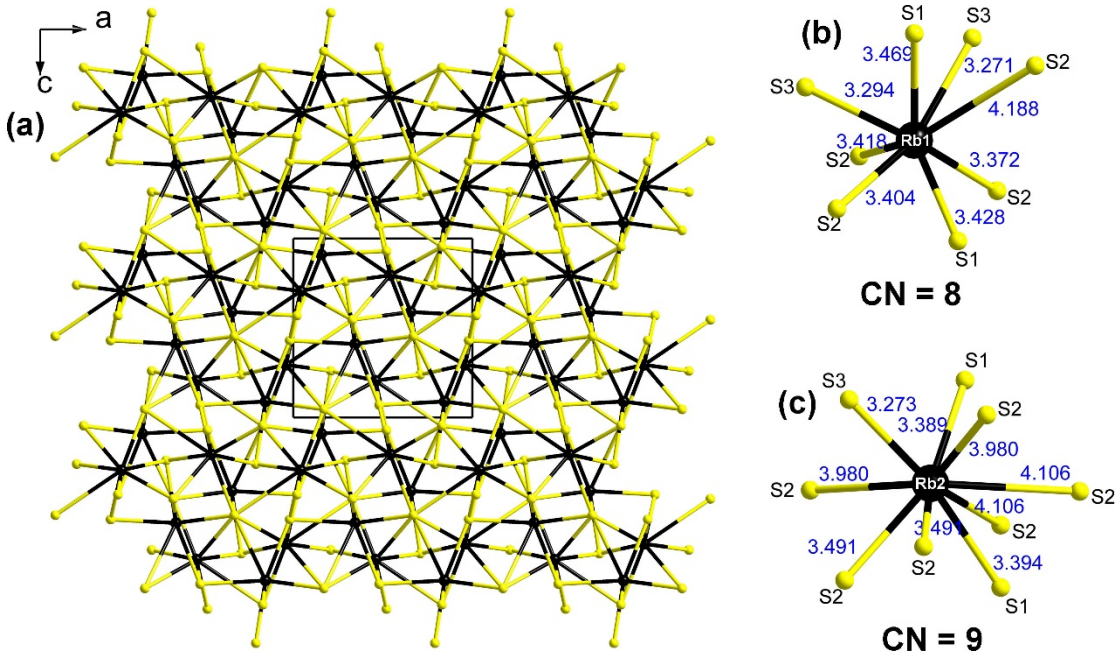

Figure S2. (a) 3D Rb–S framework and (b, c) coordination environment and bond lengths (Å) of crystallographic independent Rb atoms in Rb_3PS_4.

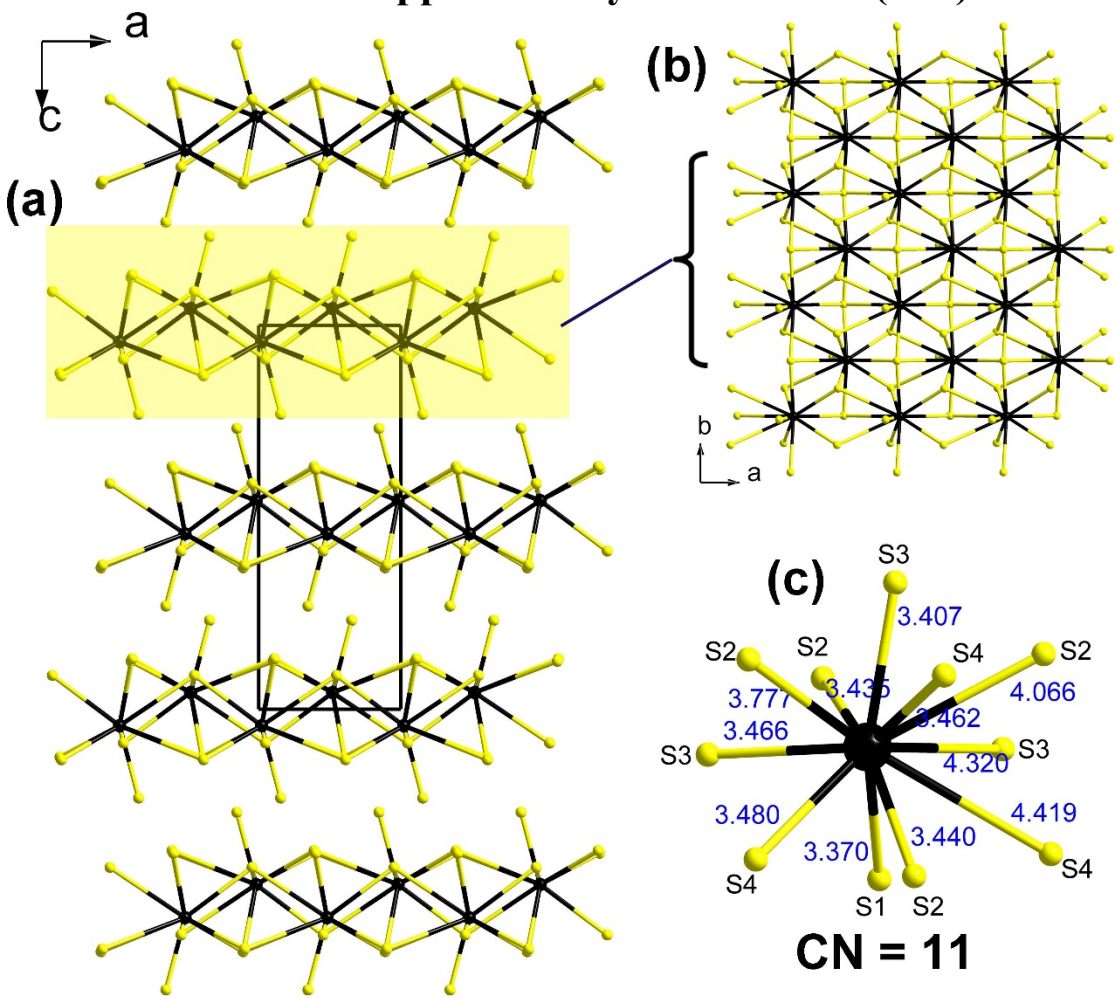

Figure S3. (a, b) 2D Rb–S layer and (c) coordination environment and bond lengths (Å) of crystallographic independent Rb atoms in $RbPbPS_4$.

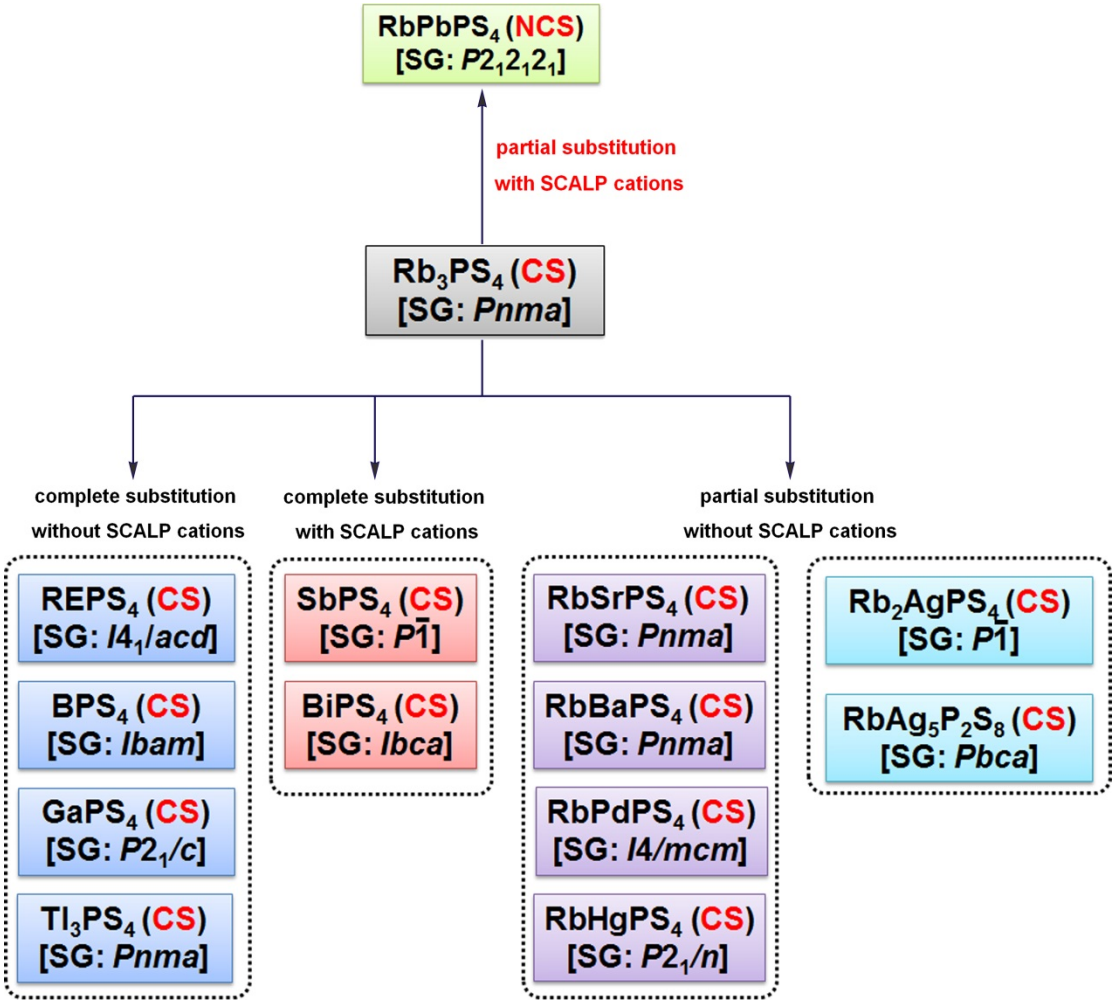

Figure S4. Detailed structural evolution between known ternary and quaternary chalcophosphates through chemical substitution.

Electronic Supplementary Information (ESI)

Table S1. Crystallographic data and refinement details for $RbPbPS_4$.

Empirical formula	$RbPbPS_4$
CCDC number	2347371
Formula weight	451.87
Temperature (K)	293(2)
Crystal system	orthorhombic
Space group	$P2_12_12_1$ (No.19)
a (Å)	6.3981(2)
b (Å)	6.6888(2)
c (Å)	17.2823(5)
V (Å^3)	739.61(4)
Z	4
D_c (g·cm^{-3})	4.058
μ (mm^{-1})	30.577
GOOF on F^2	1.064
R_1, wR_2 ($I > 2\sigma(I)$) [a]	0.0220, 0.0528
R_1, wR_2 (all data)	0.0226, 0.0530
Largest diff. peak and hole (e·Å^{-3})	1.636, –1.057

[a]: $R_1 = \Sigma||F_o| - |F_c||/\Sigma|F_o|$, $wR_2 = [\Sigma w(F_o^2 - F_c^2)^2/\Sigma w(F_o^2)^2]^{1/2}$

Table S2. Selected bond lengths (Å) and angle (°) of $RbPbPS_4$.

Pb–S1	2.931(3)	∠S1–Pb–S1	81.59(5)
Pb–S1	3.087(2)	∠S1–Pb–S3	96.08(8)
Pb–S2	2.916(2)	∠S1–Pb–S4	147.26(8)
Pb–S3	2.994(3)	∠S1–Pb–S4	129.85(6)
Pb–S3	2.994(3)	∠S1–Pb–S4	87.15(8)
Pb–S4	3.040(3)	∠S2–Pb–S1	70.66(7)
Pb–S4	3.114(3)	∠S2–Pb–S1	85.42(7)
P–S1	2.069(3)	∠S2–Pb–S3	149.76(7)
P–S2	2.033(3)	∠S2–Pb–S4	85.08(8)
P–S3	2.031(4)	∠S2–Pb–S4	135.66(7)
P–S4	2.036(4)	∠S3–Pb–S1	65.41(7)
		∠S3–Pb–S4	94.22(8)
		∠S3–Pb–S4	67.50(6)
		∠S4–Pb–S1	74.68(7)
		∠S4–Pb–S4	125.42(4)
		∠S2–P–S1	111.04(15)
		∠S2–P–S4	109.79(15)
		∠S3–P–S1	106.56(15)
		∠S3–P–S2	111.62(16)
		∠S3–P–S4	108.39(16)
		∠S4–P–S1	109.34(15)

Electronic Supplementary Information (ESI)

Table S3. Atomic coordinates and equivalent isotropic displacement parameters of $RbPbPS_4$.

Atom	*Wyckoff*	*x*	*y*	*z*	U_{eq}(Å)[a]
Rb	4*a*	0.48039(17)	0.50355(14)	0.54314(5)	0.0162(3)
Pb	4*a*	0.78872(6)	0.47458(6)	0.76936(2)	0.01095(16)
P	4*a*	0.2803(4)	0.5107(3)	0.84832(14)	0.0075(5)
S1	4*a*	0.3462(4)	0.5316(3)	0.73141(14)	0.0111(5)
S2	4*a*	0.5473(4)	0.5040(4)	0.91204(13)	0.0105(5)
S3	4*a*	0.1009(5)	0.7515(3)	0.87519(16)	0.0117(7)
S4	4*a*	0.1102(5)	0.2587(3)	0.86839(16)	0.0107(6)

U_{eq} is defined as one third of the trace of the orthogonalized U_{ij} tensor.

Electronic Supplementary Information (ESI)

Table S4. Properties comparison of the reported Pb-based IR-NLO chalcogenides.

Number	Formula	Space group	E_g (eV)[a]	d_{eff}[b] (× $AgGaS_2$)	LIDT (× $AgGaS_2$)	Δn	Ref.
1	$Pb_4Ga_4GeSe_{12}$	$P\bar{4}2_1c$	1.19	2	N/A[c]	0.0504	15
2	$Pb_{0.72}Mn_{2.84}Ga_{2.95}Se_8$	$P\bar{6}$	1.65	4.4	N/A	N/A	16
3	$PbGa_2GeSe_6$	$Fdd2$	1.96	5	3.7	0.114	17
4	$PbGa_2SiSe_6$	Cc	2.17	N/A	N/A	0.087	17
5	$Pb_{0.65}Mn_{2.85}Ga_3S_8$	$P\bar{6}$	2.25	1.5	N/A	N/A	16
6	$Pb_5Ga_6ZnS_{15}$	$Ama2$	2.32	N/A	N/A	0.1137	18
7	$Pb_4Ga_4GeS_{12}$	$P\bar{4}2_1c$	2.35	N/A	N/A	N/A	15
8	β-$PbGa_2S_4$	$Pna2_1$	2.46	0.1	3.0	0.04	19
9	$[Na_2PbI][Ga_7S_{12}]$	$Imm2$	2.53	4.5	3.6	0.069	20

10	$[K_2PbX][Ga_7S_{12}]$ (X = Cl/Br/I	*Imm*2	2.41-2.54	2.5-2.7	2.3-4.0	N/A	21
11	$Pb_{3.5}GeS_4Br_3$	$P6_3$	2.6	0.8	3.0	0.131	22
11	Pb_4SeBr_6	*Fdd*2	2.62	1.3	10	0.127	23
12	**$RbPbPS_4$**	**$P2_12_12_1$**	**2.79**	**3.2**	**7.5**	**0.109**	**this work**
13	$PbGa_4S_7$	*Pc*	3.08	1.2	N/A	N/A	24

Electronic Supplementary Information (ESI)

4 References

1 P. Kubelka and F. Munk, Reflection characteristics of paints, *Z. Techn. Phys.*, 1931, **12**, 593−601.

2. CrystalClear Version 1.3.5 Rigaku Corp.: Woodlands, TX, 1999.

3. P. Kubelka, Ein beitrag zur optik der farbanstriche, *Z. Tech. Phys.*, 1931, **12**, 593–601.

4. S. K. Kurtz and T. T. Perry, A powder technique for the evaluation of nonlinear optical materials, *J. Appl. Phys.*, 1968, **39**, 3798−3813.

5. M. J. Zhang, X. M. Jiang, L. J. Zhou and G. C. Guo, Two phases of Ga_2S_3: promising infrared second-order nonlinear optical materials with very high laser induced damage thresholds, *J. Mater. Chem. C*, 2013, **1**, 4754–4760.

6. G. Kresse, VASP, 5.3.5 http://cms.mpi.univie.ac.at/vasp/vasp/vasp.html.

7. G. Kresse and J. Furthmuller, Efficient iterative schemes for ab initio total-energy calculations using a plane-wave basis set, *Phys. Rev. B: Condens. Matter*, 1996, 11169–11186.

8. G. Kresse and D. Joubert, From ultrasoft pseudopotentials to the projector augmented-wave method, *Phys. Rev. B: Condens. Matter*, 1999, **59**, 1758–1775.

9. Blochl, P. E. Projector augmented-wave method, *Phys. Rev. B: Condens. Matter*, 1994, **50**, 17953–17979.

10 J. P. Perdew, K. Burke and M. Ernzerhof, Generalized gradient approximationmade simple, *Phys. Rev. Lett.*, 1996, **77**, 3865–3868.

11. D. J. Chadi, Special points for Brillouin-zone integrations, *Phys. Rev. B: Condens. Matter*, 1978, **16**, 1746–1747.

12. Z. Fang, J. Lin, R. Liu, P. Liu, Y. Li, X. Huang, K. Ding, L. Ning and Y. Zhang, Computational design of inorganic nonlinear optical crystals based on a genetic algorithm, *CrystEngComm.*, 2014, **16**, 10569–10580.

13. C. Aversa and J. E. Sipe, Nonlinear optical susceptibilities of semiconductors: Results with a length-gauge analysis, *Phys. Rev. B*, 1995, **52**, 14636–14645.

14. S. N. Rashkeev, W. R. L. Lambrecht and B. Segall, Efficient ab initio method for the calculation of frequency-dependent second-order optical response in semiconductors, *Phys. Rev. B*, 1998, **57**, 3905–3919.

15. Y. K. Chen, M. C. Chen, L. J. Zhou, L. Chen and L. M. Wu, Syntheses, Structures, and Nonlinear Optical Properties of Quaternary Chalcogenides: $Pb_4Ga_4GeQ_{12}$ (Q = S, Se), *Inorg. Chem.*, 2013, **52**, 8334–8341.

16. M. Zhou, X. Jiang, Y. Guo, Z. Lin, J. Yao and Y. Wu, $Pb_{0.65}Mn_{2.85}Ga_3S_8$ and $Pb_{0.72}Mn_{2.84}Ga_{2.95}Se_8$: Two Quaternary Metal Chalcognides with Open-Tunnel-Framework Structures Displaying Intense Second Harmonic Generation Responses and Interesting Magnetic Properties, *Inorg. Chem.*, 2017, **56**, 8454–8461.

17. Z. Z. Luo, C. S. Lin, H. H. Cui, W. L. Zhang, H. Zhang, H. Chen, Z. Z. He and W. D. Cheng, $PbGa_2MSe_6$ (M = Si, Ge): Two Exceptional Infrared Nonlinear Optical Crystals, *Chem. Mater.*, 2015, **27**, 914–922.

18. R. H. Duan, J. S. Yu, H. Lin, Y. J. Zheng, H. J. Zhao, S. X. Huang-Fu, M. A. Khan, L. Chen and L. M. Wu, $Pb_5Ga_6ZnS_{15}$: a noncentrosymmetric framework with chains of T_2-supertetrahedra, *Dalton Trans.* 2016, **45**, 12288–12291.

19. W. F. Chen, B. W. Liu, X. M. Jiang and G. C. Guo, Infrared nonlinear optical performances of a new sulfide β-$PbGa_2S_4$, *J. Alloy. Compd.*, 2022, **905**, 164090.

20. Z. X. Wu, W. F. Chen, X. M. Jiang, B. W. Liu and G. C. Guo, $[Na_2PbI][Ga_7S_{12}]$: Combining Diamond-Like Anionic Framework with Polycationic Chain toward

Achieving Remarkable Nonlinear Optical Response, *Chem. Mater.*, 2024, **36**, 3444–3451.

21. W. F. Chen, B. W. Liu, S. M. Pei, X. M. Jiang and G. C. Guo, $[K_2PbX][Ga_7S_{12}]$ (X = Cl, Br, I): The First Lead-Containing Cationic Moieties with Ultrahigh Second-Harmonic Generation and Band Gaps Exceeding the Criterion of 2.33 eV, *Adv. Sci.*, 2023, **10**, 2207630.

22. J. Zhou, H. Wang, J. Liu, X. Su, Y. Chu, J. Qu and X. Jiang, $Pb_{3.5}GeS_4Br_3$: The first phase-matching thiogermanate halide infrared nonlinear optical material, *Inorg. Chem. Front.*, 2024, DOI: 10.1039/d4qi00293h.

23. J. Wang, H. Wu, H. Yu, Z. Hu, J. Wang and Y. Wu, Pb_4SeBr_6: A Congruently Melting Mid-Infrared Nonlinear Optical Material with Excellent Comprehensive Performance, *Adv. Optical Mater.*, 2022, **10**, 2102673.

24. X. Li, L. Kang, C. Li, Z. Lin, J. Yao and Y. Wu, $PbGa_4S_7$: a wide-gap nonlinear optical material, *J. Mater. Chem. C*, 2015, **3**, 3060–3067.